

Performance improvement of seismic-isolated bridges near active faults using elastic-gap devices

M. Dicleli

Department of Engineering Sciences, METU, Ankara, Turkey



2017 NZSEE
Conference

ABSTRACT: For seismic isolated bridges (SIBs) subjected to near-fault (NF) ground motions with directivity effect, the isolator displacements tend to be considerably large. Consequently, isolators with very large dimensions may be required for SIBs located in NF zones. This may lead to very large expansion joints and very large seat widths as well. In this research, the efficiency of providing supplemental elastic-gap devices to improve the performance of seismic-isolated bridges (SIBs) in near-fault (NF) zones is investigated. The device is primarily made of elastomeric bearings placed in parallel with seismic isolators to provide additional elastic stiffness upon closure of a gap. A parametric study, involving more than 400 nonlinear time history (nonlinear time-history) analyses of realistic and simplified structural models of typical SIBs are conducted using simulated and actual NF ground motions to investigate the applicability of the proposed solution. It is found that providing elastic-gap device is beneficial in reducing the isolator displacements to manageable ranges. It is also found that the gap and the stiffness of the elastic-gap device may be chosen in relation to the magnitude of the NF ground motion to minimize the isolator displacements by moving away from the high-energy region of the spectrum. Further analyses conducted using a realistic structural model of an existing bridge and five NF earthquakes with moderate to large magnitudes confirmed that elastic-gap device may be used to reduce the displacement of the isolators while keeping the substructure base shear forces at practically acceptable ranges for SIBs located in NF zones.

1 INTRODUCTION

For seismic isolated bridges (SIB) subjected to far-field ground motions, the isolator displacements is generally in an economically feasible range (Dicleli & Buddaram 2006). However, for SIBs subjected to NF ground motions with directivity effect, the isolator displacements tend to be considerably large (Liao et al. 2004). Thus, isolators, expansion joints and substructures with very large dimensions may be required for SIBs located in NF zones to accommodate such large isolator displacements. Consequently, the application of seismic isolation to bridges in NF zones becomes virtually impractical as a stand-alone seismic mitigation technique (Liao et al. 2004). Although it may be possible to reduce the isolator displacements and shear forces to manageable ranges by providing additional seismic control devices, most of such devices are generally expensive and are not commonly used for seismic protection of bridges, mainly due to the lack of experience with such devices and the associated maintenance cost. Thus, a rational solution to the problem associated with large isolator displacements for SIBs subjected to NF earthquakes is required.

To address the problem stated above, the efficiency of using elastic gap devices (EGD) in SIBs for reducing the isolator displacements while keeping the shear forces at practically acceptable ranges for a wide range of NF ground motion magnitudes is investigated. Elastomeric bearings placed in parallel with seismic isolators between the superstructure and substructures that are engaged upon closure of a gap may be used for this purpose. Elastomeric bearings have already been used over many years by state departments of transportation and require only minimal initial cost and maintenance compared to most seismic control devices. Thus, they can easily be used for seismic design and retrofitting of SIB located in NF zones.

2 CONFIGURATION AND BEHAVIOUR OF EGD FOR BRIDGES

A typical configuration of isolators and EGDs in a common type of SIB with slab-on-girder deck is displayed in Figure 1 (a). In the figure, while the isolators are placed underneath the girders, the EGDs are mounted underneath the diaphragms over the substructures using usual construction techniques. In this type of a configuration, the isolators underneath the girders are designed to carry the gravity loads.

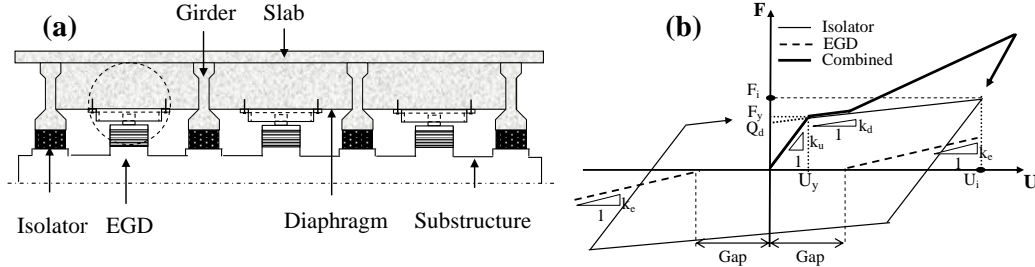


Figure 1. (a) Typical configuration of isolator and elastic-gap device (b) Force displacement relationships of isolator, elastic-gap device and their combination.

Figure 1(b) illustrates the idealized force-displacement hysteresis relationship of a typical isolator and an EGD considered in this study. In the figure, Q_d , k_u , k_d , F_y , u_y , F_i and u_i are respectively the characteristic strength, elastic stiffness, post-elastic stiffness, yield force, yield displacement, maximum (or design) force and displacement of the isolator respectively, while k_e is the stiffness of the EGD that is engaged upon closure of the gap. The thick solid line in the figure demonstrates the combined force-displacement relationship of the isolator and the EGD.

3 DESIGN AND PERFORMANCE PHILOSOPHY OF THE EGD

A SIB equipped with EGDs is expected to function at two seismic performance levels based on the magnitude of the NF ground motion. For small magnitude NF earthquakes where the isolator displacements are within practical ranges, the gap of the EGDs is designed to be larger than the displacement of the isolators. Accordingly, under the effect of such earthquakes, the gap of the EGDs is not closed and the elastomeric bearings are not engaged in resisting the movement of the SIB superstructure. This is anticipated to result in smaller forces transferred to the substructures. However, under large magnitude NF earthquakes, the isolator displacements are expected to be quite large, so that the gap of the EGDs is closed and the elastomeric bearings are engaged in resisting the movement of the SIB superstructure. This is expected to reduce the isolator displacements to manageable ranges but amplify the shear forces to some extent. However, in spite of the amplified shear forces, the EGDs, when applied to SIBs, are expected to produce a more practical and economical seismic design or retrofitting solution due to the considerable reductions in isolator displacements.

4 NEAR- FAULT GROUND MOTIONS CONSIDERED

Two sets of NF ground motions are considered. The first set involves a suite of 36 simulated NF ground motions used to study the effect of EGDs on the performance of SIBs in relation to NF ground motion properties. The simulation is performed for moment magnitudes (M_w) ranging between 6.0 and 7.5 and fault distances (r) ranging between 3 and 18 km. For the assumed range of M_w and r , the peak ground velocity, V_p , and the velocity pulse period, T_p , of the simulated NF ground motions are obtained using the following relationships (Somerville 1998);

$$\ln(V_p) = -2.31 + 1.15M_w - 0.5\ln(r) \quad (1)$$

$$\text{Log}_{10}(T_p) = -2.5 + 0.425M_w \quad (2)$$

For the simulation of velocity and acceleration time histories of the NF ground motions, the following

relationships presented by Agrawal and He (2002) are used

$$\dot{u}_g = se^{-\zeta_p \omega_p t} \sin \omega_p \sqrt{1 - \zeta_p^2} t \quad (3)$$

$$\ddot{u}_g = se^{-\zeta_p \omega_p t} \left(-\zeta_p \omega_p \sin \omega_p \sqrt{1 - \zeta_p^2} t + \omega_p \sqrt{1 - \zeta_p^2} \cos \omega_p \sqrt{1 - \zeta_p^2} t \right) \quad (4)$$

where ζ_p is the decaying factor, ω_p is the frequency of the sinusoid, s is the initial amplitude of the velocity pulse and t is the time in seconds.

The second set of ground motions contains five NF earthquakes (Table 1). In this table, A_p indicates the peak ground acceleration. The rest of notations used in this table are previously defined. These earthquakes are used for the verification of the results obtained using simulated NF ground motions.

Table 1. Important features of earthquake records used in the analyses.

Earthquake	Station	M_w	r (km)	A_p (g)	V_p (cm/s)	T_p (s)
Northridge, 1994	Rinaldi	6.7	7.1	0.84	166.1	1.25
Loma Prieta, 1989	Gilroy, Arr. #02,	6.9	12.7	0.32	39.1	1.40
Northridge, 1994	Sylmar, Olive View H.,	6.7	6.1	0.84	116.3	2.60
Imperial Valley, 1979	Elcentro, Array # 05,	6.5	1.0	0.38	90.5	3.90
Landers, 1992	Lucerne, SCE Sta. 24,	7.3	1.1	0.72	97.6	5.00

5 ANALYSES CONDUCTED AND PARAMETERS CONSIDERED

Nonlinear time history analyses are conducted in two phases to study the effect of EGDs on the performance of SIBs. In the first phase, a parametric study, involving more than 400 nonlinear time history analyses of simplified structural models representative of typical SIBs, are performed using simulated NF ground motions. As the response of SIBs subjected to pulse type excitations are governed by the mass, m , of the bridge, the properties, Q_d , k_d , of the isolator and the properties, M_w and r (or V_p and T_p), of the NF ground motion, the effect of EGDs on the performance of SIBs is considered in relation to these parameters and the EGD properties (gap and elastic stiffness). For this purpose, a total of ten different combinations of isolator-EGD stiffness values and gap openings are considered. Furthermore, the analyses are performed for Q_d/W ratios ranging between of 0.025 and 0.15 where W is the tributary weight acting on the isolator. In the second phase of analyses, the results obtained from simplified structural models and simulated NF ground motions are verified. For this purpose an actual bridge with (i) regular elastomeric bearings (ii), with isolators and (iii) with isolators and EGDs is modelled and analysed using five recorded NF ground motions.

6 ANALYSES WITH SIMULATED NF GROUND MOTIONS

6.1 Properties of the simplified SIBs used in the analyses

The effect of the EGD on the performance of SIBs is studied by considering a typical SIB with $Q_d/W=0.05$ ($W=2000$ kN, $Q_d=100$ kN) and post-elastic stiffness producing a post-elastic period of $T_s=4.01$ s.

6.2 Simplified structural models of typical SIBs with and without EGD

The simplified structural models used for nonlinear time history analyses are built using the program SAP2000 (2005). In the models, the substructure stiffness is not considered and the bridge superstructure is assumed to have infinite in-plane rigidity. Accordingly, for the SIB without the EGD, the structural model is simplified as a tributary rigid mass directly connected to a nonlinear SAP2000 link (isolator) element with bilinear force-displacement relationship (Fig. 2 (a)).

For the simplified SIB model with the EGD, two L-shaped rigid bars are connected to the base of the isolator element as shown in Figure 2(b). Two nonlinear link-gap elements defined by an elastic stiffness and a gap in SAP2000 are then connected between the top of the isolator element and the L-shaped rigid bars to simulate the behaviour of the EGD in an actual bridge.

6.3 Behaviour of the SIB with and without the EGD

The behaviour of a SIB with and without EGDs subjected to NF ground motions with $M_w=6.0$, $r=6$ km and $M_w=7.5$, $r=6$ km is compared in Figs 3 (a) and (b) respectively. Each figure displays the isolator velocity time history and shear force versus isolator displacement hysteretic behavior. The EGD used in the analyses has an elastic stiffness, $k_e=2k_d$ and a gap=10 cm.

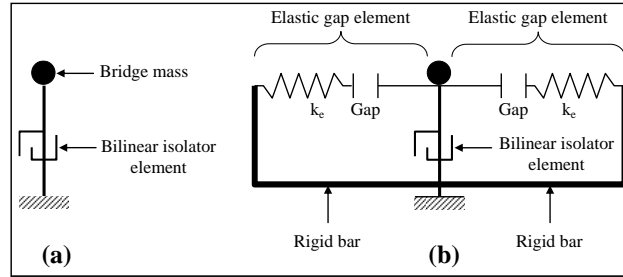


Figure 2. Simplified structural models of (a) SIB, (b) SIB with EGD.

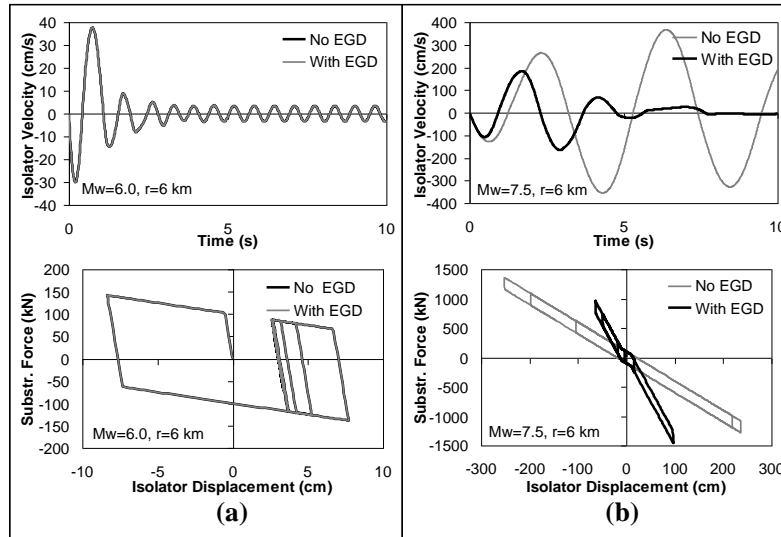


Figure 3. Comparison of the velocity time histories and isolator force- displacement hysteretic behaviours of a regular SIB and a SIB with EGD for NF ground motions with (a) $M_w=6$, $r=6$ km (b) $M_w=7.5$, $r=6$ km.

As observed from Figure 3(a), for NF ground motions with small magnitude, the behaviour of the SIB with and without the EGD overlap since the 8.22 cm maximum isolator displacement is smaller than the 10 cm gap of the EGD. Thus, the EGD is not engaged in resisting the movement of the isolator for small magnitude NF earthquakes as intended in design. However, as observed from Figure 3(b), for NF ground motions with large magnitudes, the EGD is engaged in limiting the displacement of the isolators. The 252 cm maximum isolator displacement is reduced to 105 cm when an EGD is used. However, the 1361 kN force transferred to the substructure of the SIB is increased to 1453 kN due to the presence of the EGD. Nevertheless, the 6.8% increase in the shear force is negligible compared to the dramatic, 58.3%, reduction in the isolator displacement. More importantly, as observed from the isolator's displacement and velocity time histories of Figure 3(b), using an EGD in the SIB results in smaller isolator velocities and a faster decay of the isolator displacement and velocity amplitudes. This is very beneficial for the cyclic performance of the isolators as the heat generated by the isolators under cyclic motion will be noticeably reduced due to the presence of the EGD.

6.4 Effect of EGD on bridge performance for various gap openings

The effect of the EGD on the performance of SIBs is first studied by varying the gap of the EGD between 0 and 40 cm while keeping its stiffness at $k_e=5k_d$. Fig 4 (a) displays the variation of the isolator displacement as a function of M_w at $r=6$ km for a regular SIB and a SIB with an EGD with gaps=0, 5, 10, 20, 30 and 40 cm. As observed from the figure, the EGD is very beneficial for reducing the isolator displacements for all the values of gaps considered. Furthermore, the benefits of using EGDs become more pronounced at large NF ground motion magnitudes and smaller gap openings. Figure 4 (b) displays the variation of the shear force as a function of the magnitude of the simulated NF ground motions for a regular SIB and a SIB with an EGD having various gaps. As observed from the figure, the reduction in the isolator displacements due to the EGD comes at the expense of some increase in the shear forces. The difference between the shear forces of the cases with and without the EGD is more noticeable for NF ground motions with moderate to large magnitudes ($M_w \leq 7.2$) and larger gap sizes (gap ≥ 20). For SIBs with EGDs, larger gap sizes result in shear forces comparable to those of the regular SIBs for small magnitude NF ground motions and larger than those of the regular SIBs for large magnitude NF ground motions. However, using EGD may still be beneficial due to the significant reduction in isolator displacements. The smallest possible gap size should be chosen for the EGD based on the maximum ID of a regular SIB subjected to the SDL earthquake. This will ensure a satisfactory performance of the SIB with EGD under both SDL and MCDL earthquakes.

6.5 Effect of EGD on bridge performance for various elastic stiffness values

In this section, the effect of the EGD on the performance of SIBs is studied by varying the stiffness of the EGD ($k_d \leq k_e \leq 9k_d$). For all the EGD stiffness values, the gap of the EGD is kept at 20 cm. Fig 4 (c) displays the variation of the ID as a function of M_w at $r=6$ km for a regular SIB and a SIB with an EGD with $k_e=k_d, 3k_d, 5k_d, 7k_d$ and $9k_d$. As observed from the figure, the EGD effectively reduces the IDs for all the stiffness values considered. The benefits of using EGDs to reduce the isolator displacements are observed to become more pronounced at larger k_e and M_w values ($M_w \geq 6.9$). But, even at very small k_e values (e.g. $k_e=k_d$) the reduction in the isolator displacements is significant. Nevertheless, as observed from Figure 4(d), larger k_e values produce larger shear forces in comparison to that of the regular SIB especially at smaller NF ground motion magnitudes. Thus, the stiffness of the EGD must be kept at a minimum to obtain practically acceptable levels of shear forces at small NF ground motion magnitudes while effectively reducing the isolator displacements at large NF ground motions.

6.6 EGD versus fault distance

In this section, the effect of the EGD on the seismic performance of SIBs is studied in relation to the distance from the fault. For this purpose, the seismic performance of a regular SIB and a SIB bridge with various EGD properties is compared for various fault distances. The analyses results are presented in Figure 5(a). The figure displays the isolator displacements and shear forces as a function of M_w for $r=6, 12$ and 18 km. As observed from the figure, the beneficial effects of the EGD on the seismic performance of SIBs are more pronounced for smaller fault distances. It is also observed that at further fault distances, introducing an EGD produces shear forces comparable to those of the regular SIB at smaller NF ground motion magnitudes. Nevertheless, the analyses results show that using EGD is beneficial for reducing the isolator displacements regardless of the distance from the fault.

6.7 EGD versus characteristic strength of isolator

In this section, the effect of the EGD on the seismic performance of SIBs is studied in relation to the characteristic strength of the isolator. Figure 5(b) display the isolator displacement and shear force of a regular SIB and a SIB with EGDs with various elastic stiffness values and gap openings as a function of M_w for $Q_d/W = 0.05, 0.10$ and 0.15 and $r=6$ km. As observed from the figure, using EGD is generally beneficial for reducing the isolator displacements for the range of Q_d/W ratios considered in this study. However, using EGDs with a small elastic stiffness in combination with isolators with higher characteristic strength generally produce shear forces comparable to those of the regular SIB and a practically acceptable reduction in isolator displacements for all the range of NF ground motion magnitudes considered.

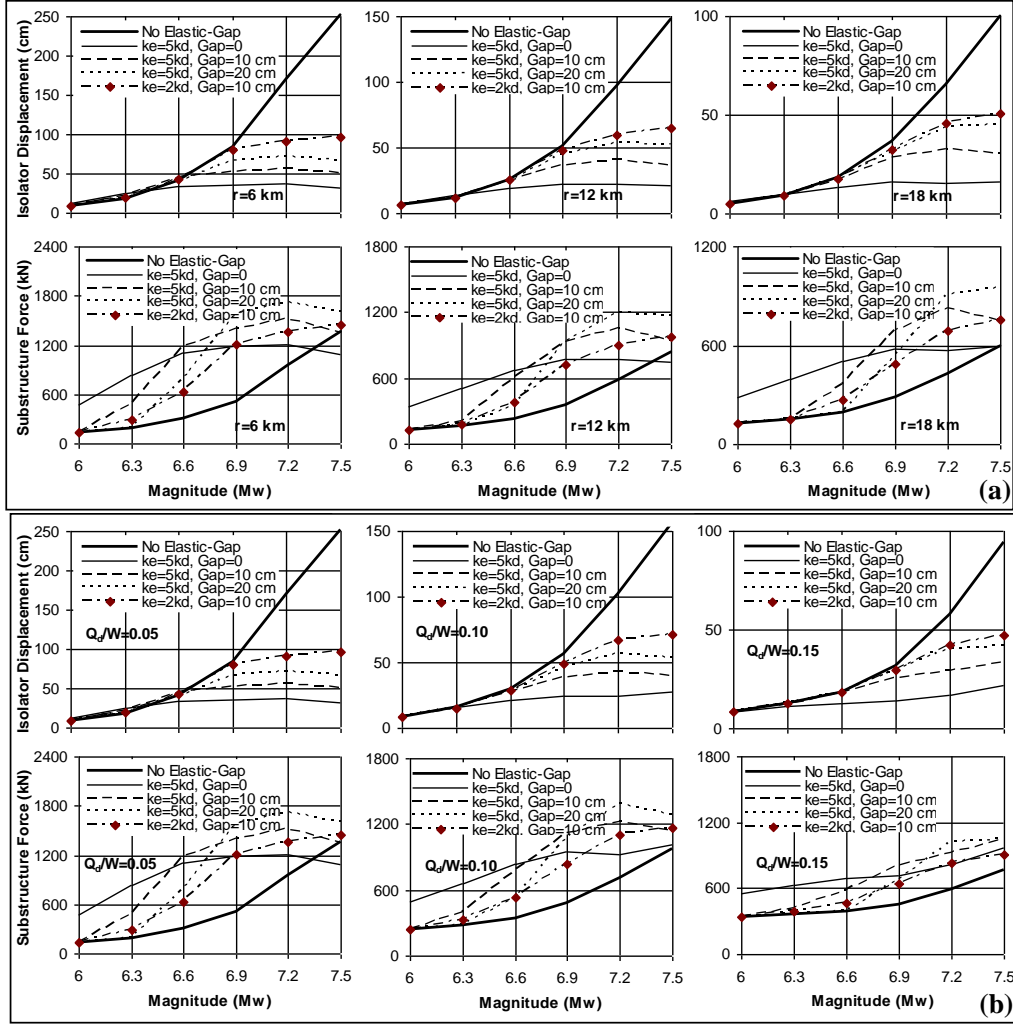


Figure 5. (a) Isolator displacement and shear force versus ground motion magnitude for various fault distances (b) Isolator displacement and shear force versus ground motion magnitude for various isolator characteristic strength values.

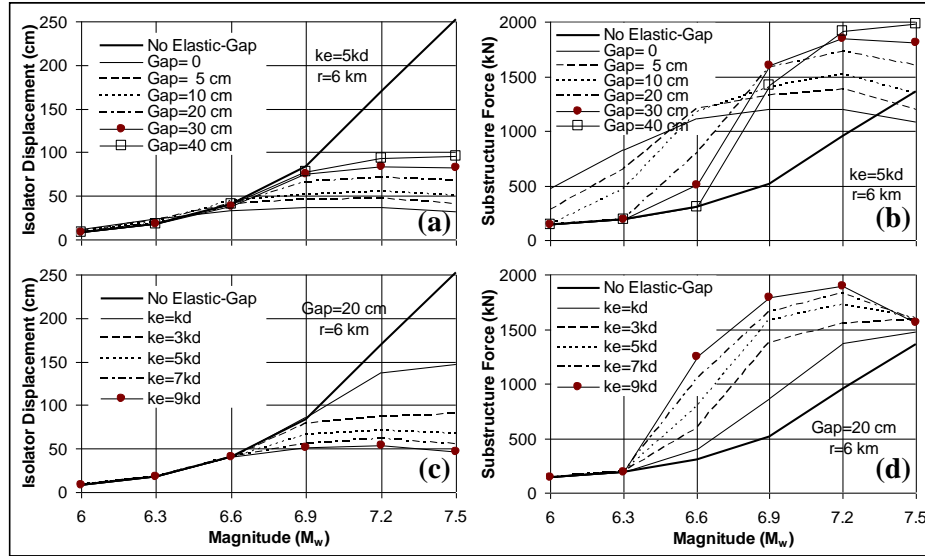


Figure 4. (a) Effect of EGD gap on isolator displacement (b) Effect of EGD gap on substructure force (c) Effect of EGD stiffness on isolator displacement (d) Effect of EGD stiffness on substructure force.

7 ANALYSIS RESULTS WITH AN ACTUAL SIB AND NF EARTHQUAKES

In this section, the results obtained from the nonlinear time history analyses of simplified structural models representing SIBs and SIBs with EGDs are verified using an actual bridge located in South Central US. The nonlinear time history analyses of the bridge are conducted five times in both orthogonal directions of the bridge for the regular bridge (no isolators), the bridge with isolators alone (regular SIB) and the bridge with isolators and EGDs together for three EGD gap-stiffness values. The bridge has three continuous spans and a slab-on-prestressed-concrete-girder deck as shown in Figure 6 (a). The piers are reinforced concrete multiple circular column bents. In the original bridge, laminated elastomeric bearings with 203x356x67 mm dimensions are provided underneath each girder at both abutments and Pier 1, whereas plain elastomeric bearings with 152x356x13 mm dimensions are provided at Pier 2 to provide fixity. The seismic-isolated version of the bridge has six isolators with $Q_d=10$ kN and $k_d=60$ kN/m over each substructure. Four EGDs with (i) $k_e=200$ kN/m, gap=8 cm (ii) $k_e=400$ kN/m, gap=8 cm and (iii) $k_e=800$ kN/m, gap=12 cm are provided underneath the diaphragms at both abutments and piers. A detailed 3-D structural model of the bridge shown in Figure 6(b) is built using the program SAP2000. Nonlinear soil bridge interaction effects are simulated in the structural model. The bridge superstructure is modelled using 3-D beam elements. The behaviour of the isolators is modelled using a nonlinear isolator link element with bilinear force deformation relationship. The behaviour of the EGDs is modelled using a nonlinear link gap element with an elastic stiffness and a gap opening. The piers are modelled using 3-D beam elements and the abutments are modelled using a grid of 3-D beam elements as illustrated in Figure 6 (b). The soil-bridge interaction at the abutments is included in the model using boundary elements attached at the interface nodes between the abutment, backfill and the piles as shown in Figure 6 (b). Details about superstructure, substructure and soil-bridge interaction modeling can be found elsewhere (Dicleli and Hindi 2005).

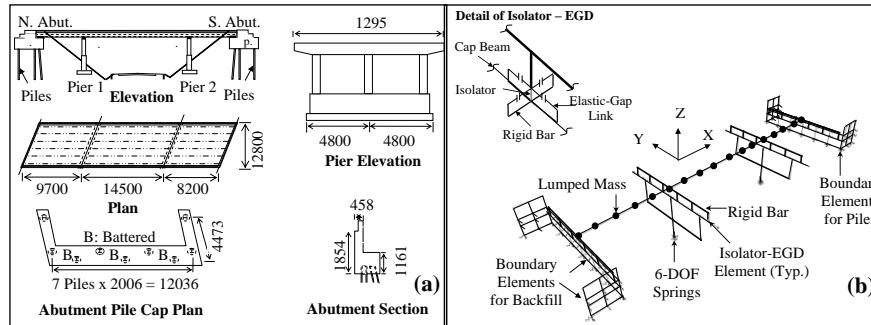


Figure.6. (a) Details of the bridge (dimensions are in mm), (b) Structural model of the bridge.

7.1 Analysis results

The analyses of the bridge are conducted using the five NF earthquakes presented in Table 1, representing MCDL earthquakes and using the same earthquakes scaled by a factor of 0.5 representing SDL earthquakes. The analyses are conducted for the following five cases (i) the original (regular) bridge with elastomeric bearings (ii) SIB, (iii) SIB with 4 EGDs; $k_e=200$ kN/m, gap=8 cm, (iv) $k_e=400$ kN/m, gap=8 cm, (v) $k_e=800$ kN/m, gap=12 cm. The analyses results for the longitudinal and transverse directions are similar. Thus, only the results for the longitudinal direction are presented in Figures. 7 (a)-(d). Figure 7 (a) displays the isolator displacements for the bridge subjected to the MCDL earthquakes. Figure 7 (b) is similar but presents the analysis results for the same bridge subjected to the SDL earthquakes. Figures. 7 (c) and (d) display Pier 1 (Pier 2 is similar) base shear forces for MCDL and SDL earthquakes respectively. However, the analyses results for the regular bridge (case (i)) are presented for both Piers 1 and 2 due to the difference in the base shear forces. It is observed from Figures. 7 (a) and (c) that introducing EGDs resulted in a considerable reduction in the displacements while the shear forces are kept at practically acceptable ranges at the MCDL earthquakes. As expected, for the SDL earthquakes (Figs. 7(b) and (d)), the displacements and shear forces for the SIB with EGD remained similar to those of the regular SIB. For the SIB with EGD subjected to the MCDL earthquakes however, displacements as low as 55 percent of those of the

regular SIB are obtained. In spite of the notable reduction in the displacements, the average shear forces remained at only 59 to 64 percent of those of the original bridge without seismic-isolation depending on the properties of the EGD used.

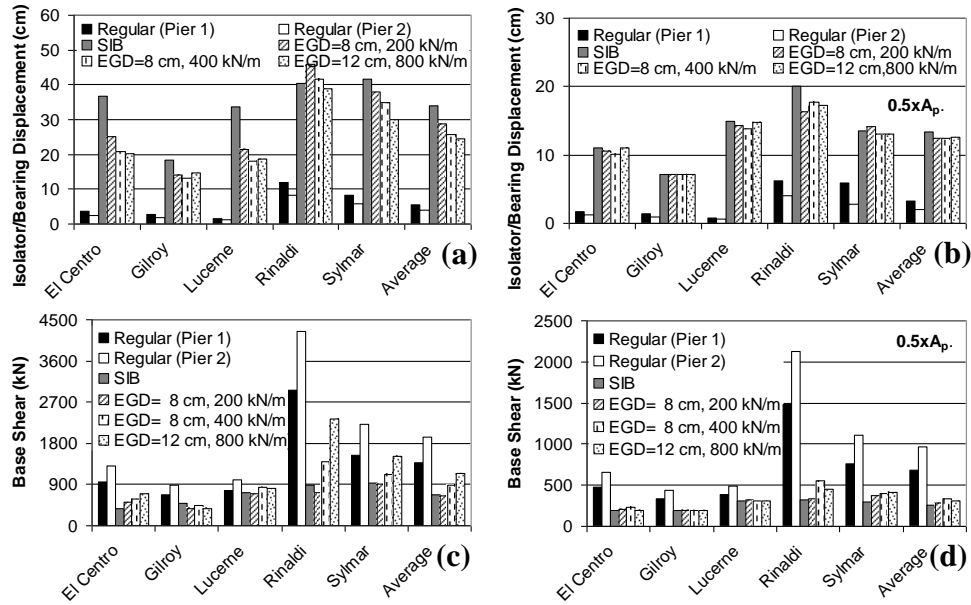


Figure 7. Longitudinal direction seismic response of the bridge at the piers, (a) Isolator displacements for the MCDL earthquake, (b) Isolator displacements for the SDL earthquakes (c) Pier base shear forces for the MCDL earthquakes, (d) Pier base shear forces for the SDL earthquakes.

8 CONCLUSIONS AND RECOMMENDATIONS

In this paper, the efficiency of using EGDs in SIBs for reducing the isolator displacements at MCDL earthquakes while keeping the shear forces at practically acceptable ranges at SDL and MCDL earthquakes is investigated. It is found that EGDs produced displacements and shear forces comparable to those of the regular SIBs at the SDL earthquakes. However, at the MCDL earthquakes, EGDs reduced the displacements to practically manageable ranges while keeping the shear forces within practically acceptable limits regardless of the distance from the fault and the properties of the isolator. Additionally, using EGDs produced smaller isolator velocities and a faster decay of the displacement and velocity amplitudes of the isolator. This is very beneficial for the cyclic performance of the isolators as the heat generated by the isolators under cyclic motion will be dramatically reduced due to the presence of the EGDs. It may be recommended that for the performance based design and retrofitting of SIBs using EGDs under SDL and MCDL NF earthquakes, the smallest possible gap size should be chosen for the EGD based on the maximum displacement of a regular SIB subjected to the SDL earthquake. Moreover, the stiffness of the EGD must be kept at a minimum level based on the extent of displacement reduction required in a particular design or retrofitting application. This will ensure a satisfactory performance of the SIB with EGD under both SDL and MCDL earthquakes.

9 REFERENCES, SYMBOLS AND UNITS

- Agrawal, A.K. & He, W.L. (2002). A closed-form approximation of near-fault ground motion pulses for flexible structures, *Proceedings of Engineering Mechanics Conference, American Society of Civil Engineers*.
- Dicleli, M. & Buddaram, S. (2006). Effect of isolator and ground motion characteristics on the performance of seismic-isolated bridges. *Earthquake Engineering and Structural Dynamics* 35(2): 233-250.
- Dicleli, M. & Hindi, R. (2005). Seismic retrofitting of bridges by response modification techniques based on altering bearing fixities. *Journal of Earthquake Engineering*; 9(4):483-495.
- Liao, W.I., Loh, C.H. & Lee, B.H. (2004). Comparison of dynamic response of isolated and non-isolated continuous girder bridges subjected to near-fault ground motions. *Engineering Structures* 26(14): 2173-2183.